Astron. Astrophys. 243, 429–444 (1991)

ASTRONOMY AND ASTROPHYSICS

The winds of O-stars

III. A comparison between observed and predicted degrees of ionization in the winds of O-stars

M.A.T. Groenewegen[1] and H.J.G.L.M. Lamers[1,2]

[1] SRON Laboratory for Space Research, Sorbonnelaan 2, NL-3584 CA Utrecht, The Netherlands
[2] Astronomical Institute at Utrecht, Princetonplein 5, NL-3584 CC Utrecht, The Netherlands

Received June 26, 1989; accepted June 11, 1990

Abstract. The results of the UV linefitting of 26 O-stars and one B0 supergiant were used to compare the observed degrees of ionization in the winds with the predicted ionization for wind models calculated by Pauldrach (1987), Pauldrach et al. (1989) and Drew (1989). We have compared the empirical ionization structure in the entire wind for a few stars with the detailed models. For all our sample stars we compared empirical ionization ratios (e.g. N v/C IV, Si IV/C IV, N IV/N V) with their predicted values at $v=0.5\,v_\infty$.

Both comparisons led to the same conclusion as to the origin of the large discrepancies, up to factors 10^2 to 10^3, between predictions and observations.

In general both sets of theoretical calculations predict too much ionization. They underestimate the Si IV abundance and overestimate the C IV abundance at low effective temperatures. The N V abundance is overestimated for stars earlier than O7, but underestimated at O8 and later. The latter effect is the well known superionization. Both sets of theoretical calculations do not take Auger-ionization by X-rays into account which in principle might explain the presence of N V at low effective temperatures.

Key words: lines: profile – stars: circumstellar matter – early type – mass-loss – UV radiation

1. Introduction

All studies intended to derive the mass loss from hot stars on the basis of the UV line profiles suffer from the uncertainty in the degree of ionization and excitation in the stellar winds. That the ionization balance cannot be explained by a simple equilibrium with the photospheric radiation has been clear since the discovery of ions like O VI and N V in the UV spectra of stars with types as late as B3 (Snow & Morton 1976). Several explanations have been proposed to account for the presence of these super-ions: a warm wind of a few hundred thousand Kelvin (Lamers & Morton 1976; Lamers & Rogerson 1978; Lamers & Snow 1978), Auger-ionization, by X-ray's either from a thin corona at the base of the wind (Olson 1978; Cassinelli & Olson 1979; Waldron 1984) or from X-rays produced in shocks (Lucy 1982) and photoionization from excited levels (Pauldrach 1987). Cassinelli et al. (1978) argued against a warm wind model on the basis of their fit to the Hα profiles in ζ Ori and ζ Pup. They found that the mass loss needed to explain the Hα profiles would exceed the single scattering limit $\dot{M}_{\max}=L/v_\infty c$ if the wind temperature was $T=2\,10^5$ K. An important argument in favour of the explanation of the superionization by Auger-ionization, i.e. two-electron ionization, is the observation that O VI occurs in the winds of stars in which Oxygen is mainly O IV, N V occurs when nitrogen is mainly N III etc. (Cassinelli & Olson 1979).

The discovery of X-rays from hot stars (Harnden et al. 1979; Long & White 1980; Cassinelli et al. 1981; Cassinelli & Swank 1983) has made the Auger-effect even more plausible for explaining superionization. Baade & Lucy (1987) showed that the source of the X-rays cannot be a thin corona at the base of the wind because of the absence of the Fe XIV 5303 Å coronal emission line. Moreover, a detailed study of the X-ray spectrum of a few O-type stars by Cassinelli & Swank (1983) shows that at least part of the observed X-ray flux must be generated throughout the wind, rather than at the base of the wind. Therefore it is most likely that the X-rays are created in shocks occurring in the entire wind. It has been shown that the X-ray spectrum resulting from such a model (Lucy 1982) is in accordance with observations if one assumes the presence of some strong shocks (Cassinelli & Swank 1983).

Linear stability analyses have convincingly shown that a line-driven wind is unstable and it is therefore thought that such instabilities will eventually result in shocks which heat the gas (Lucy & Solomon 1970; MacGregor et al. 1979; Martens 1979; Carlberg 1980; Lucy 1984; Owocki & Rybicki 1984, 1985, 1986). Recently Owocki et al. (1989) have shown that the non-linear time dependent evolution of instabilities can qualitatively explain various observational properties of O stars, e.g. enhanced infrared emission due to clumping in the wind and the presence of narrow absorption components.

An alternative explanation of the superionization has been proposed by Pauldrach (1987). He claimed that the problem of superionization was only artificial and that it has arisen only because the calculations so far did not include the full multilevel NLTE calculations. He found that low lying levels were collisionally excited and subsequently photoionized to higher stages than without collisional excitation. For ζ Pup he could explain the presence of N V and O VI in the wind. However, Drew (1989) found that the electron temperature in the wind is lower ($T_e \simeq 0.6 T_{\rm eff}$) than previously assumed in ionization calculations ($T_e \simeq 0.8-1.0\,T_{\rm eff}$) by e.g. Pauldrach (1987), because of the cooling from lines of abundant metals. This will decrease the

Send offprint requests to: H. Lamers (first address above)

importance of photoionization from collisionally excited levels. It is obvious that both Auger-photoionization by X-rays and photoionization from excited levels are important in determining the ionization balance in the wind. Unfortunately calculations including both effects have yet to be performed. This implies that all studies using UV lines as a mass loss indicator have used wrong (warm wind model, X-rays from a corona) or incomplete (neglecting Auger-ionization or ionization from excited levels), physical models to calculate the ionization balance. Therefore the mass loss rates derived from UV lines with theoretical ionization fractions may be seriously in error.

We have undertaken an effort in studying the stellar wind of O-stars by means of a detailed analysis of the UV lineprofiles of 26 O-stars and one B0-supergiant. The observations are from the most accurate data set available up to now, i.e. the Atlas of IUE high resolution spectra of O-type stars by Walborn et al. (1985). The observed profiles were fitted with theoretical profiles calculated with the SEI method (Lamers et al. 1987) in which the formation of doublets and the effects of photospheric absorption lines and turbulence in the wind is taken into account. The analysis and the line fits are described in Paper I of this series (Groenewegen & Lamers 1989a). The agreement between the observed and predicted profiles is very good in most cases. The resulting terminal velocities of the winds of O-stars were studied in Paper II (Groenewegen et al. 1989b).

In this study we will derive the empirical ionization fractions for the few stars in our sample for which accurate mass loss determinations exist from radio measurements. Furthermore, we will compare the observed ionization ratios, q_i/q_j, for different combinations of ions with the predicted ones of the grid of models of Pauldrach (1987), Pauldrach et al. (1989) and those of Drew (1989). For a few stars we will compare the observed and predicted variation of $\dot{M}q$ (mass loss times ionization fraction) with distance in the wind. This may lead to constraints on the origin of the discrepancies between observed and predicted ionization fractions.

2. The ionization in the winds derived from the UV lines

2.1. The method

Paper I of this series was devoted to the analyses of the P Cygni profiles of 26 O and one early B star observed in the UV by the IUE satellite. The lines studied are the resonance lines of C IV (1548, 1550 Å), N V (1238, 1242 Å) and Si IV (1393, 1402 Å) and the subordinate lines of C III (1175 Å) and N IV (1718 Å). It was shown that the adopted fits matched the observed line profiles very well in most cases.

The program stars and their basic data are described in Table 1. The compilation of these data is described in Paper II. The adopted temperature scale and the bolometric corrections are from Chlebowski & Garmany (1989) based on NLTE studies of a number of O-stars. The absolute visual magnitudes are from the compilation of Garmany (1987) which is predominantly based on cluster membership. The masses are derived from $T_{\rm eff}$ and L and the evolutionary tracks of Maeder & Meynet (1987). We assumed that the stars are moving away from the main sequence, rather than returning from the Red Supergaint Phase. The radii are derived from L and $T_{\rm eff}$. The Newtonian gravity and the escape velocity corrected for radiation pressure by electron scattering are also given.

The significant improvement in the overall quality of the fits compared to linefits made with the Sobolev approximation (compare e.g. our fits (Paper I) with those of Olson & Castor 1981) is largely due to the fact that we used the SEI method (Lamers et al. 1987) which accounts for the presence of a turbulent velocity in the wind. In this method the source function is calculated using the Sobolev approximation with escape probabilities, but the transfer equation is solved exactly. Lamers et al. (1987) have shown that the SEI method, which is based on a suggestion by Hamann (1981), is almost as accurate as the more physical correct Comoving Frame Method (CMF) but it is much more efficient, so it can be used to fit line profiles almost interactively.

In Paper I we derived the following relation between the mass loss and ionization fraction and the derived fit parameters:

$$\dot{M}q_i(w)E_i(w) = 1.189\ 10^{-18}\ R_*\, v_\infty^2\, (f\, A_E\, \lambda_0)^{-1}\, \{\tau(w) x^2 w\, dw/dx\}, \tag{1}$$

with $\dot{M}$ in $M_\odot\ \mathrm{yr}^{-1}$, R_* in $R_\odot$, v_∞ in $\mathrm{km\,s}^{-1}$ and λ_0 in Å. E_i represents the excitation fraction of the lower level of the observed transition, f the oscillator strength, A_E the abundance by number relative to H, for which we used the values of Palme et al. (1982), x is the normalised radial coordinate $x = r/R_*$, w is the normalised velocity $w = v/v_\infty$ and τ represents the radial optical depth law for which we assumed

$$\tau(w) = \begin{cases} \dfrac{T}{I}\left(\dfrac{w}{w_1}\right)^{\alpha_1}\left(1-\left(\dfrac{w}{w_1}\right)^{1/\beta}\right)^{\alpha_2} & w_0 \leqslant w \leqslant w_1 \\ 0 & w_1 < w \leqslant 1. \end{cases} \tag{2}$$

The total optical depth T is related to the total column density N_i of the absorbing ion.

$$T = \int_{w_0}^{1} \tau(w)\, dw = (\pi e^2/mc)\, f\lambda_0 N_i \tag{3}$$

I is a normalization constant

$$I = \int_{w_0}^{w_1} (w/w_1)^{\alpha_1}\, \{1-(w/w_1)^{1/\beta}\}^{\alpha_2}\, dw. \tag{4}$$

The parameter w_1 represents the maximum velocity to which the ion was observed. This particular choice of $\tau(w)$ was justified in Paper I. We adopted a velocity law of the type

$$w(x) = w_0 + (1-w_0)\,(1-1/x)^{\beta} \tag{5}$$

with $w_0 = 0.01$ and with β and v_∞ as free parameters. The values of the optical depth parameters T, α_1, α_2 and of the velocity law v_∞, β and of $v_{\rm turb}$ were derived from the line fitting (Paper I). The values of v_∞, β and $v_{\rm turb}$ are listed in Table 1.

2.2. The variation of ionization and excitation through the wind

From the parameters described above the values of $\dot{M}q_i(w)E_i(w)$ can be derived for each ion and each star. In Figs. 1 and 2 we plotted for a number of stars the value of $\dot{M}q_i(w)E_i(w)$ for the resonance line of C IV, N V and Si IV which have $E_i(w) \simeq 1$, and for the excited lines of C III′ and N IV′ (the prime indicates excited lines). In Table 2 we collected for all our sample stars the values of $\dot{M}q_iE_i$ at $w = 0.5$, together with their errors. For saturated lines only -3σ lower limits are given. Although we did not plot error bars in Figs. 1 and 2 for clarity purposes, it should be noted that the errors in the values of $\dot{M}q_iE$ are larger at small ($w \leqslant 0.2$) and

Table 1. The program stars

HD	Name	Type	log T_{eff} (K)	log L ($L_\odot$)	log R ($R_\odot$)	log M ($M_\odot$)	log g (cm s^{-2})	v_{esc} (km s^{-1})	v_∞ (km s^{-1})	β	v_{turb} (km s^{-1})
93250		O3 V((f))	4.686	6.08	1.19	1.92	3.98	1120	3300 ± 200	0.7 ± 0.1	260 ± 80
93129A		O3 If*	4.648	6.13	1.29	1.92	3.78	960	3050 ± 60	0.9 ± 0.1	180 ± 80
46223		O4 V((f))	4.667	5.70	1.04	1.73	4.09	1190	2800 ± 60	0.6 ± 0.1	200 ± 90
164794	9 Sgr	O4 V((f))	4.667	6.02	1.20	1.87	3.91	1060	2950 ± 150	0.9 ± 0.1	210 ± 60
66811	ζ Pup	O4 I(n)f	4.627	5.87	1.20	1.77	3.81	970	2200 ± 60	0.7 ± 0.1	290 ± 70
190429A		O4 If$^+$	4.627	6.03	1.28	1.85	3.73	920	2300 ± 70	0.9 ± 0.1	370 ± 140
15629		O5 V((f))	4.646	5.72	1.09	1.72	3.98	1090	2900 ± 70	0.7 ± 0.1	150 ± 80
46150		O5 V((f))	4.646	5.72	1.09	1.72	3.98	1090	2900 ± 200	0.7 ± 0.1	200 ± 90
93204		O5 V((f))	4.646	5.48	0.97	1.62	4.12	1170	2800 ± 60	0.5 ± 0.1	360 ± 80
15558		O5 III(f)	4.626	6.03	1.29	1.85	3.71	910	3350 ± 200	0.7 ± 0.1	110 ± 90
14947		O5 If$^+$	4.605	5.85	1.24	1.74	3.70	890	2300 ± 70	0.7 ± 0.1	230 ± 100
101190		O6 V((f))	4.625	5.74	1.14	1.71	3.87	1010	2900 ± 150	0.8 ± 0.1	170 ± 80
210839	λ Cep	O6 I nfp	4.582	5.87	1.29	1.75	3.61	850	2100 ± 60	0.6 ± 0.1	210 ± 70
101436		O6.5 V	4.615	5.60	1.09	1.64	3.90	1010	2800 ± 150	0.5 ± 0.25	220 ± 80
190864		O6.5 III(f)	4.593	5.62	1.15	1.62	3.76	910	2450 ± 150	0.5 ± 0.15	125 ± 100
163758		O6.5 Iaf	4.571	5.96	1.36	1.77	3.49	760	2200 ± 70	0.5 ± 0.1	260 ± 140
47839	15 Mon	O7 V((f))	4.603	5.29	0.96	1.54	4.06	1110	2300 ± 200	0.5 ± 0.1	320 ± 110
24912	ζ Per	O7.5 III(n)((f))	4.569	5.32	1.04	1.50	3.86	950	2400 ± 100	0.5 ± 0.15	290 ± 120
188001	9 Sge	O7.5 Iaf	4.545	5.90	1.38	1.72	3.40	710	1800 ± 70	1.2 ± 0.2	250 ± 90
101413		O8 V	4.580	5.23	1.12	1.48	3.68	860	2900 ± 200	0.6 ± 0.1	580 ± 290
36861	λ Ori	O8 III((f))	4.556	5.36	1.09	1.51	3.77	900	2400 ± 150	0.5 ± 0.1	290 ± 70
151804		O8 Iaf	4.532	6.14	1.53	1.84	3.22	600	1600 ± 70	1.0 ± 0.1	240 ± 80
37043	ι Ori	O9 III	4.532	5.58	1.25	1.59	3.53	790	2450 ± 150	0.6 ± 0.1	370 ± 70
30614	α Com	O9.5 Ia	4.490	5.95	1.52	1.71	3.11	560	1550 ± 60	0.7 ± 0.1	190 ± 60
37742	ζ Ori	O9.7 Ib	4.484	5.74	1.42	1.61	3.21	620	2100 ± 150	0.7 ± 0.1	320 ± 130
149038	μ Nor	O9.7 Iab	4.484	5.70	1.40	1.58	3.22	610	1750 ± 100	0.7 ± 0.1	260 ± 150
37128	ε Ori	B0 Ia	4.447	5.80	1.53	1.62	3.00	630	1500 ± 150	0.7 ± 0.1	230 ± 80
Typical uncertainties: (dex)			0.02	0.20	0.14	0.10	0.2	0.15			

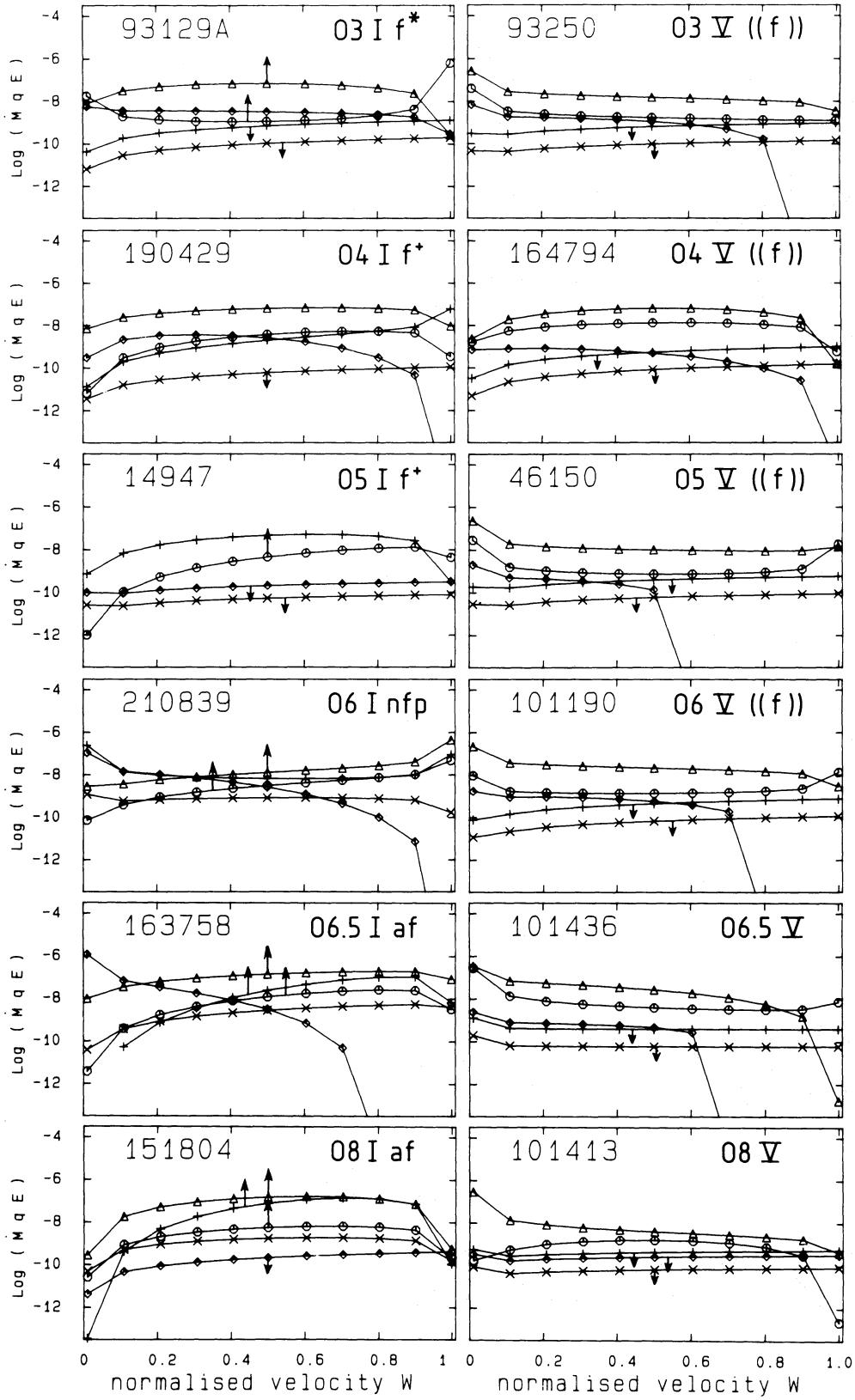

Fig. 1. Value of $\dot{M}qE(w)$ for a sample of representative supergiants and main sequence stars of types O3 to O8 for the ions we considered. The following symbols are used: C IV (○), N V (△), Si IV (+), C III (×), N IV (◇). Lower limits are indicated by an arrow of length 1.3 dex. The length of the arrow of the upper limits has no specific meaning

large velocities ($w \geq 0.9$). In most cases the error in $\dot{M}q_iE_i$ reaches a minimum in the range $w = 0.40$–0.60, where the typical error is 0.2 dex. For both $w \simeq 0.1$ and $w \simeq 0.9$ we find a typical error of 0.37 dex. It was argued in Paper I that in the case of a saturated line an upperlimit of roughly 20 times the lower limit can be imposed on the value of the integrated optical depth T, and therefore on $\dot{M}qE$, because, given the uncertainty in the other parameters, no acceptable fit could be found for too large values

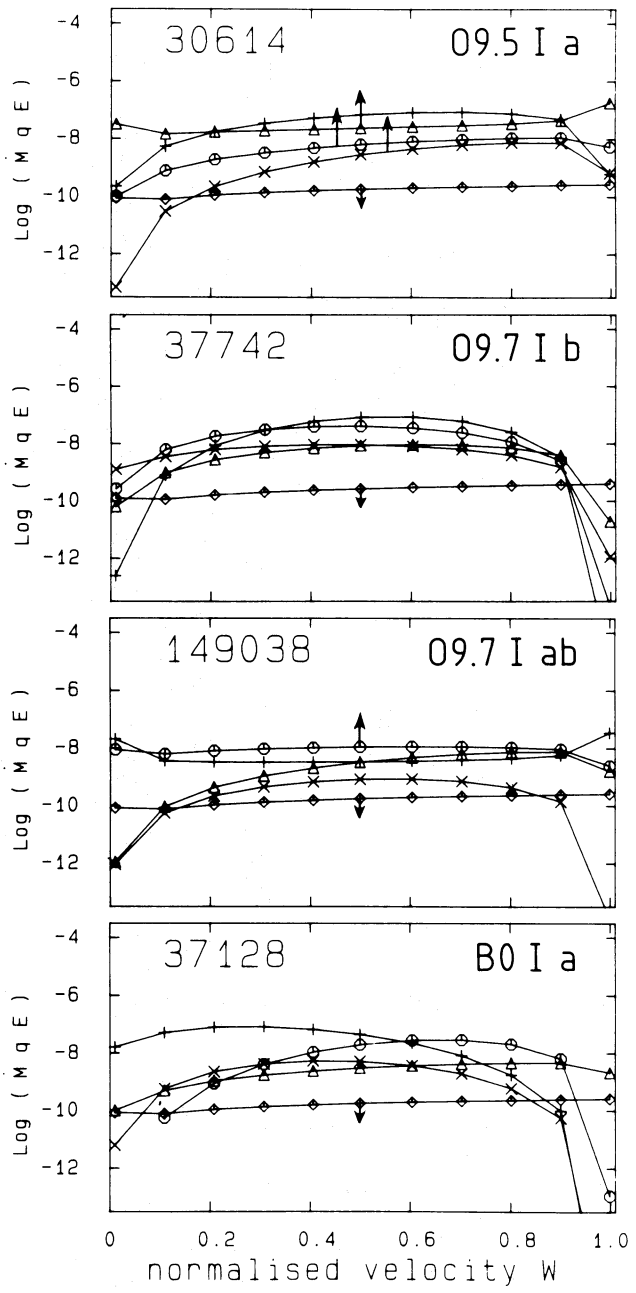

Fig. 2. Same as Fig. 1 but for supergiants of type O9.5 and later

of T. This factor of 20 (1.3 dex) corresponds to the length of the arrows indicating the upperlimits in Figs. 1 and 2.

Figure 1 shows the variation of $\dot{M}q_i(w)E_i(w)$ with w for a sample of representative supergiants and main sequence stars of types O3 to O8. The cooler supergiants are shown in Fig. 2. For the stars not shown in this figure, the values of $\dot{M}q_i(w)E_i(w)$ can easily be derived from the values of the line-fit parameters given in Paper I (Table 4). The following conclusions can be drawn from these figures. a) The values of $\dot{M}q_i$ for C IV, N V and Si IV derived from their resonance lines are remarkably constant throughout the range of $0.2 < w < 0.9$. (The decrease or increase at $w \leq 0.2$ or $w \geq 0.9$ is possibly due to the larger uncertainty mentioned above). This implies that the degrees of ionization of these ions hardly vary with distance in the wind between 1.1 and about 7 R_*. b) The value of $\dot{M}q_iE_i$ of N IV′ decreases with velocity for almost all stars of types O6.5 and earlier. This decrease is stronger at types O6–O6.5 than at earlier types. Stars of types later than O6.5 do not show the excited lines of N IV′ in the wind. c) The excited lines of C III′ are absent in the winds of all main sequence O-stars and in the winds of supergiants of types O5 and earlier, with the exception ζ Pup (not shown in Fig. 1). In those supergiants which show C III′ lines, the values of $\dot{M}q_iE_i$ are approximately constant in stars of types O8 and earlier, whereas they show a parabolic behaviour with a maximum near $w \simeq 0.5$ for the later types. For HD 30614 the value of $\dot{M}q_iE_i$ increases with w.

2.3. *The empirical ionization ratios*

Because an independent determination of $\dot{M}$ (i.e not based on the UV lines) does not exist for most of our stars, we compare the observed ionization ratios q_iE_i/q_jE_j, which are independent of $\dot{M}$, with the predicted ones, for different combinations of ions. These ratios at a velocity $w = 0.5$ are shown in Fig. 3 as a function of $T_{\rm eff}$. The following ratios are plotted: N V/C IV, Si IV/C IV, N V/Si IV, as well as C III′/C IV and N IV′/N V. The first three ratios were chosen because they are not affected by the uncertain excitation fraction and provide information about a super ion (N V) and a trace species (Si IV), the last two provide information about the relative ionization fraction for carbon and nitrogen.

There are two reasons for choosing $T_{\rm eff}$ as an independent parameter for the ionization ratios. Firstly, the observations show that the ratios are mainly dependent on $T_{\rm eff}$ with a scatter that is probably due to differences in wind densities. Secondly, the predictions by Pauldrach et al. (1989) and Drew (1989), discussed below, show that the ionization ratios are strongly dependent on $T_{\rm eff}$ and that the dependence on $\log g$ and R_* is in most cases smaller than that of $T_{\rm eff}$. The reason why a strong dependence on the ionization ratios on $T_{\rm eff}$ can be expected is based on the arguments presented in Appendix A.

Our justification of the choice of $T_{\rm eff}$ as an independent variable is confirmed by Fig. 4, where we plotted the ionization fractions of the models of Drew (1989) and Pauldrach et al. (1989) as function of $T_{\rm eff}$. We see that the ionization fractions are indeed smooth functions of $T_{\rm eff}$, and that the dependence of $\log g$ and R is in most cases small, the only exception being the carbon ionization balance at $T_{\rm eff} \simeq 30\,000$ K.

We conclude that the ionization balance in the wind is expected to depend on $T_{\rm eff}$, R and $\log g$, but that $T_{\rm eff}$ is the dominant factor. Part of the scatter which we find in the relation between ionization and $T_{\rm eff}$ is probably due to differences in wind densities. These can be taken into account in a detailed analysis of each star individually. Such an analysis is beyond the scope of this paper.

The empircial ionization ratios are plotted versus $T_{\rm eff}$ in Fig. 3.

In Fig. 3 we have highlighted by means of filled symbols or thick crosses those ratios which are not merely upper or lower limits. The dashed lines indicate mean linear relations between $\log T_{\rm eff}$ and $\log(q_i/q_j)$ or $\log(q_iE_i/q_j)$. These relations are defined by the measured values of the ionization ratios, in such a way that they are consistent with the upper or lower limits, in most cases.

Table 2. The products $\dot{M}q_i$ and $\dot{M}q_iE_i$ at $v=0.5\,v_\infty$[a]

Star HD	log $\dot{M}q_i$ C IV	log $\dot{M}q_i$ N V	log $\dot{M}q_i$ Si IV	log $\dot{M}q_iE_i$ C III'[b]	log $\dot{M}q_iE_i$ N IV'
14947	>-8.33	—	-7.32 ± 0.23	—	<-9.67
15558	>-7.36	—	<-9.08	—	-9.05 ± 0.17
15629	>-8.96	-7.41 ± 0.40	<-9.40	—	-9.31 ± 0.18
24912	>-7.90	-6.90 ± 0.41	—	-9.26 ± 0.12	-9.49 ± 0.12
30614	>-8.29	-7.62 ± 0.18	>-7.16	>-9.02	<-9.74
36861	-7.30 ± 0.19	-8.12 ± 0.15	<-9.54	-9.64 ± 0.15	<-9.76
37043	-8.46 ± 0.21	-8.13 ± 0.12	<-9.38	-9.88 ± 0.14	<-9.60
37128	-7.71 ± 0.29	-8.52 ± 0.14	-7.34 ± 0.21	-8.29 ± 0.30	<-9.75
37742	-7.39 ± 0.23	-8.03 ± 0.15	-7.07 ± 0.22	-8.04 ± 0.13	<-9.57
46150	-9.13 ± 0.13	-7.99 ± 0.13	<-9.40	—	-10.16 ± 0.12
46223	>-8.63	>-7.52	<-9.48	—	-9.46 ± 0.17
47839	-9.37 ± 0.14	-8.71 ± 0.16	<-9.71	<-10.52	<-9.92
66811	>-8.38	>-7.66	-8.56 ± 0.10	-9.31 ± 0.12	-8.40 ± 0.13
93129A	>-8.93	>-7.14	<-9.15	—	-8.50 ± 0.12
93204	>-8.69	-6.79 ± 0.31	<-9.53	—	<-9.74
93250	-8.77 ± 0.19	-7.84 ± 0.17	<-9.19	—	-9.03 ± 0.12
101190	-8.86 ± 0.14	-7.77 ± 0.18	<-9.99	<-10.81	-9.34 ± 0.13
101413	-8.79 ± 0.25	-8.39 ± 0.18	<-9.37	—	<-9.59
101436	-8.42 ± 0.22	-7.54 ± 0.19	<-9.40	—	-9.69 ± 0.17
149038	>-7.95	-8.49 ± 0.21	-8.47 ± 0.16	-9.07 ± 0.16	<-9.75
151804	>-8.25	>-6.83	>-7.10	-8.76 ± 0.27	<-9.67
163758	>-8.93	>-6.84	>-7.62	-8.55 ± 0.20	-8.64 ± 0.24
164794	-7.87 ± 0.13	-7.20 ± 0.19	<-9.27	<-10.16	-9.30 ± 0.13
188001	>-8.11	>-7.29	>-6.92	-8.77 ± 0.12	<-9.69
190429A	-8.42 ± 0.16	-7.14 ± 0.30	-8.57 ± 0.28	—	-8.60 ± 0.29
190864	>-8.35	-7.54 ± 0.23	<-9.46	—	-9.84 ± 0.21
210839	>-8.49	>-7.90	-8.18 ± 0.13	-9.08 ± 0.23	-8.58 ± 0.20

[a] All upperlimits were derived using Eq. 1 with $T<0.1$, $\alpha_1=\alpha_2=0$ and $w_1=1$

[b] In many cases the spectrum below 1200 Å was so noisy that the presence of this line could neither be confirmed nor denied. These cases are indicated by a dash

The relations are

$$\log\{\bar{q}\,(\text{N V})/\bar{q}(\text{C IV})\} \simeq -0.5+10.6\log(T_{\text{eff}}/3.10^4) \quad \text{for } 4.45\le\log T_{\text{eff}}\le 4.62$$
$$\simeq 1.0 \quad \text{for } \log T_{\text{eff}}>4.62 \tag{6a}$$

$$\log\{\bar{q}(\text{Si IV})/\bar{q}(\text{C IV})\} \simeq 0.3-2.9\log(T_{\text{eff}}/3.10^4) \text{ for class I}$$
$$\le 0.5 \quad \text{for class III, V} \tag{6b}$$

$$\log\{\bar{q}(\text{N V})/\bar{q}(\text{Si IV})\} \simeq -0.7+14.0\log(T_{\text{eff}}/3.10^4) \text{ for class I}$$
$$\ge 0.7 \quad \text{for class III, V} \tag{6c}$$

$$\log\{\bar{q}\bar{E}(\text{C III'})/\bar{q}(\text{C IV})\} \simeq -0.8-16.0\log(T_{\text{eff}}/3.10^4) \quad \text{for } 4.45\le\log T_{\text{eff}}\le 4.55$$
$$\le -1.0 \quad \text{for } \log T_{\text{eff}}>4.55 \tag{6d}$$

$$\log\{\bar{q}\bar{E}(\text{N IV'})/\bar{q}(\text{N V})\} \simeq -4.0+17.3\log(T_{\text{eff}}/3.10^4) \quad \text{for } 4.57\le\log T_{\text{eff}}\le 4.68$$
$$\le 0.5 \quad \text{for } \log T_{\text{eff}}\le 4.57. \tag{6e}$$

We stress that these are "mean relations" for our limited sample of stars. These relations describe the general trends of the ionization ratios with T_{eff}. They will be used for comparison with predicted trends. For a detailed comparison between the empirical and predicted ratios on a star to star basis, the ionization ratios can be derived from the data in Table 5 at $v=0.5\,v_\infty$ or at other velocities from the linefits presented in Paper I.

Except for the ratios Si IV/C IV and N V/Si IV, these relations have not been differentiated with respect to luminosity class, because there is no clear difference between the various luminosity classes in Fig. 3. The Si IV/C IV and N V/Si IV ratios given by Eqs. 6b and 6c are defined by three or four supergiants only. For class III and V stars we found only upper and lower limits to these ratios.

The upper and lower limits described in Eq. 6 are conservative limits: they reflect the maximum of the upper limits and the minimum of the lower limits. Stricter limits on the ionization ratios can be imposed by considering the area in the $\bar{q}_i/\bar{q}_j$ versus $\log T$ diagram (Fig. 3) covered by most of the upper and lower limits. These areas are indicated in Fig. 3 by their boundaries. Only for the Si IV/C IV ratio did we differentiate the boundaries to luminosity class. This was done because the observations indicate a strong dependence of the Si IV lines of luminosity (Sect. 3).

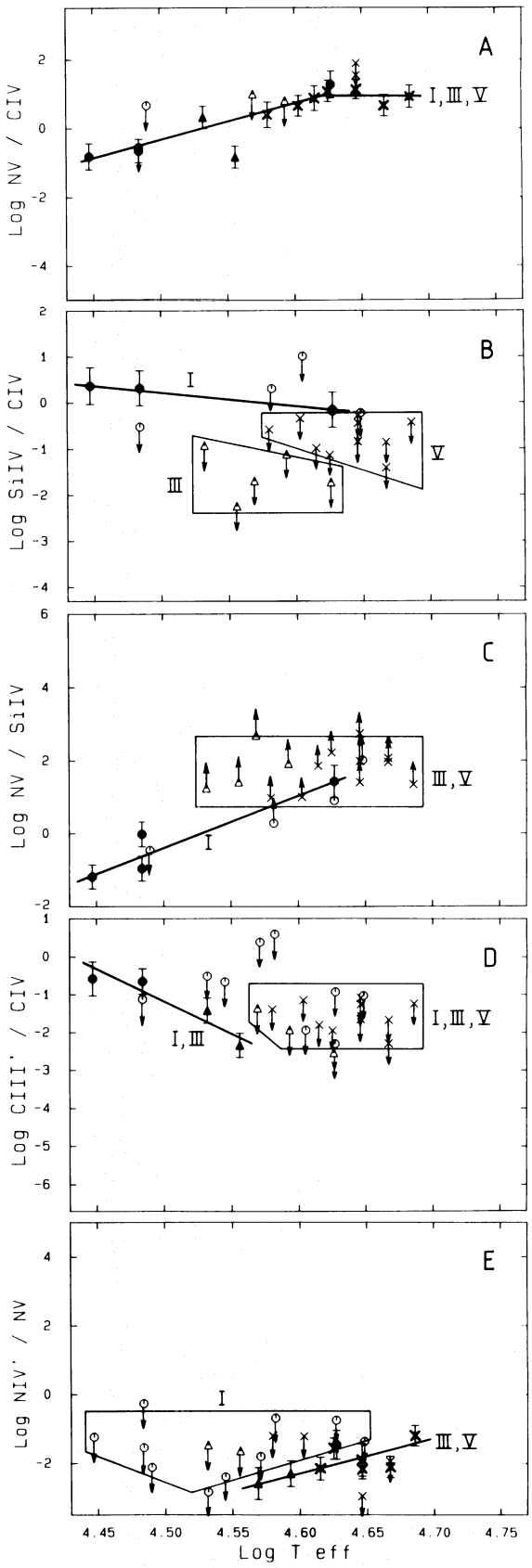

Fig. 3. Several ionization ratios at $w=0.5$ as function of temperature. We have discriminated different luminosity classes ($\bigcirc$ = I, Δ = III, $\times$ = V). Open symbols refer to upper and lower limits. The meaning of the lines and boxes is explained in the text

These ionization ratios will be compared with predictions in Sect. 3.4 and 3.5.

2.4. Observed ionization fractions derived from the UV lines and from $\dot{M}$ based on Radio observations

In this section we will derive absolute ionization fractions for the few stars for which radio mass loss determinations exist.

Mass loss observations based on radio observations have the advantage that they are model independent. Other methods depend strongly on the velocity structure at the base of the wind (IR and Hα determinations) or on the ionization structure (UV). Bieging et al. (1989) recently published a survey of radio emission at 2, 6 and 20 cm from galactic OB stars. About half of the stars detected are non-thermal emitters. One of our sample stars (9 Sgr) has been shown to be definite non-thermal emitter (Abbott et al. 1984). Six stars of our sample stars have measured radio fluxes and eight have upper limits. In Table 3 we have collected the observed radio fluxes (Abbott et al. 1980, 1981; Abbott 1985; Bieging et al. 1989), the distance (Garmany 1987; Bieging et al. 1989) and $T_{\rm eff}$ and v_∞ (Paper I), for our sample stars for which these fluxes are measured. With these values we calculated the mass loss according to:

$$\dot{M}=0.095\,\frac{\mu}{Z\gamma^{1/2}}\left(\frac{D}{\rm kpc}\right)^{3/2}\left(\frac{S_\nu}{\rm Jy}\right)^{3/4}\left(\frac{v_\infty}{\rm km\,s^{-1}}\right)(g\nu)^{-1/2}\,M_\odot\,{\rm yr}^{-1} \tag{7}$$

(Wright & Barlow 1975). Z represents the root mean square ionic charge, μ the mean molecular weight per ion and γ the mean number of electrons per ion. For these we used the values $Z=1.00$, $\mu=1.32$ and $\gamma=1.00$ respectively. These data refer to a Pop I gas in which H is fully and He is singly ionised. The gaunt factor g is evaluated using the expression given by Allen (1973)

$$g=\sqrt{3}/\pi\{17.22+\ln(T_e/\nu Z)\}, \tag{8}$$

which we evaluated at $T_e=0.5\,T_{\rm eff}$ (Drew 1989). The values of g would be about a factor 1.1 larger, and the values of $\dot{M}$ a factor 0.96 smaller if we had adopted a wind temperature of $T_e=0.8\,T_{\rm eff}$. The mass loss rates are given in Table 3. Only six stars in our sample (HD 37742 = ζ Ori, HD 37128 = ε Ori, HD 66811 = ζ Pup, HD 30614 = α Cam, HD 151804 and HD 15588) have reliable radio mass loss rates. Using these rates we calculated qE at $w=0.5$. If a star would be a nonthermal emitter the derived mass loss rate would be an upperlimit and therefore the resulting value of qE would be a lower limit.

At present, the values of q_iE_i can be compared with predictions for only one star, ζ Pup. Pauldrach (1987) calculated the ionization and excitation fractions at different distances in the wind using a Non-LTE model for the photosphere and for the wind. Our results of q(C IV), q(N V) and qE(C III′) are compared at $w=0.5$ and 0.9 with the predictions of Pauldrach's model 3, which has a slowly falling electron temperature in the wind, in Table 4. We see that at $w=0.5$ the predicted values of q(C IV) and q(N V) agree with our lower limits. The predicted value of log q(C III) = −6.2 disagrees strongly with our empirical value of log qE(C III′) = −3.9. Since the excitation fraction E is less than one, we find log q(C III) > −3.9. This lower limit is a factor ~200 higher than the prediction. This may be partly due to the fact that Pauldrach neglected dielectronic recombination, which is expected to be important for the C III/C IV ratio in the

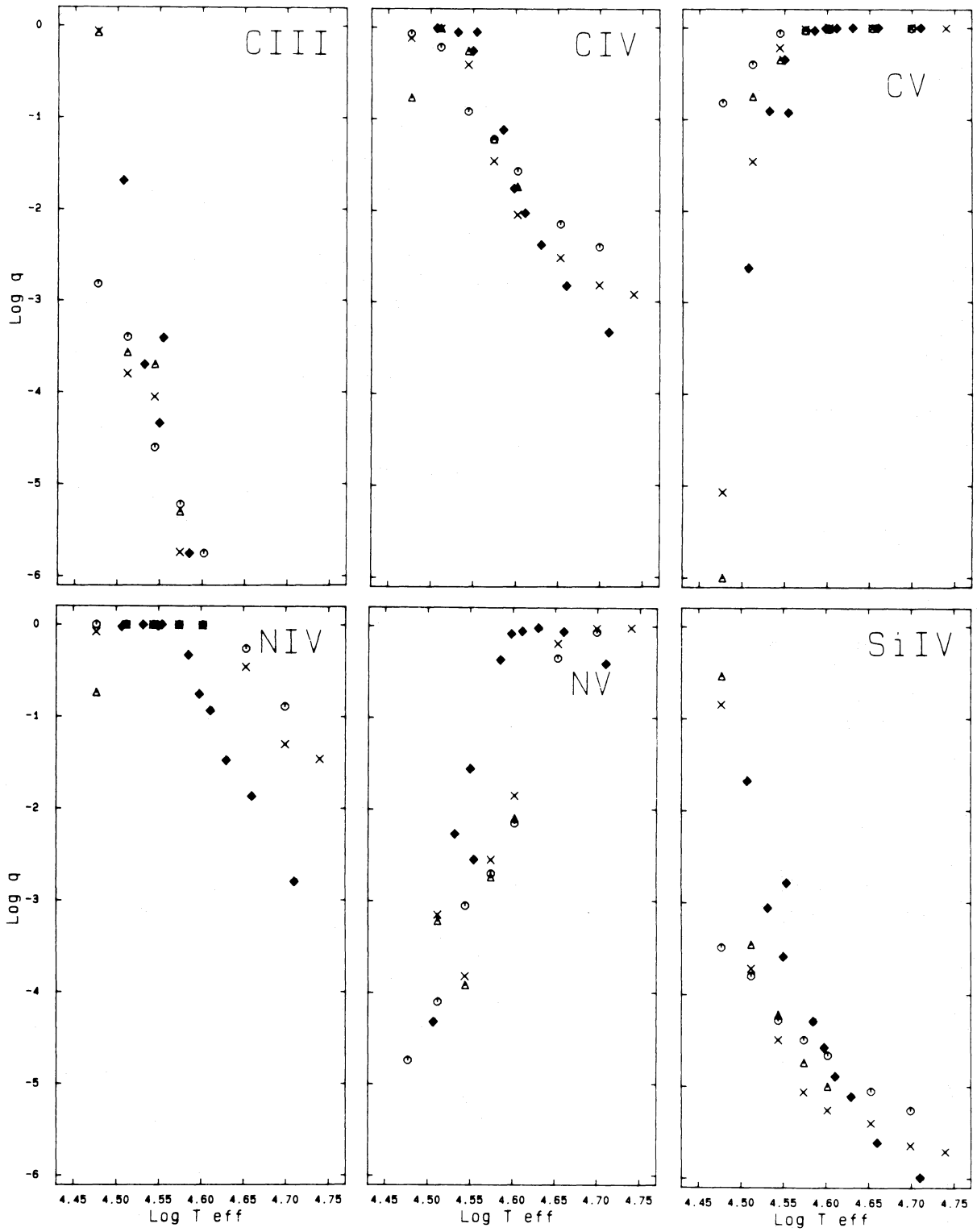

Fig. 4. Predicted ionization at $w=0.5$ for Drew's models ($\bigcirc$ = I, Δ = III, $\times$ = V) and the Munich models (filled symbols). Notice the differences up to a factor 10^3 between the two sets of models. The reason is explained in Sects. 3.1 and 3.2

wind of ζ Pup. At $w=0.9$ the discrepancy for C III is much less. This depends on the value of E we used. If we had assumed $E=0.1$ instead of $E<1$, there still would be a considerable difference. The predicted value of q(C IV) agrees with our lower limit. In Pauldrach's model, however, N V has recombined to N IV in the outer part of the wind, and the predicted value does not agree with our lower limit. This might be due to the neglect of X-rays in Pauldrach's model. Pauldrach (1987) has estimated that the Auger effect can be important, especially in the outer part of the wind.

Table 3. Mass loss determinations from radio observations

Star	D	v_∞	$T_{\rm eff}$	S(6 cm)	S(2 cm)	Ref.	Thermal	Ref.	$\dot{M}^a$	$\log qE(w=1/2)^b$				
HD	(Kpc)	(km s^{-1})	(K)	(mJy)	(mJy)		emitter		($10^{-6}\,M_\odot\,{\rm yr}^{-1}$)	C IV	N V	Si IV	C III′	N IV′
14947	2.29	2300±70	40300	<0.5	—	1	not classifiable	4	<29.4	>−3.8	—	>−2.8	—	—
15558	2.18	3350±200	42300	0.5±0.1	—	4	prob. not	4	39.6±8.7	>−3.0	—	—	—	>−4.6
30614	1.10	1550±60	30900	0.35±0.07	—	4	probable	4	5.2±1.1	>−3.9	−3.2±0.2	>−2.8	>−4.6	—
36861	0.50	2400±150	36000	<0.19	—	4	?	—	<1.53	>−1.5	>−2.3	—	>−3.8	—
37128	0.5	1500±150	28000	1.6±0.5	—	1	Probable	3	4.9±1.5	−2.4±0.3	−3.2±0.2	−2.0±0.2	−3.0±0.3	—
37742	0.44	2100±150	30500	0.7±0.2	—	1	probable	3	3.0±0.8	−1.9±0.3	−2.5±0.2	−1.6±0.2	−2.5±0.2	—
46150	1.50	2900±200	44300	<0.34	—	4	?	—	<14.6	>−4.3	>−3.2	—	—	>−5.3
46223	1.50	2800±60	46500	<0.24	—	4	?	—	<10.8	>−3.7	>−2.6	—	—	>−4.5
47839	0.69	2300±200	40100	<0.33	—	4	?	—	<3.6	>−3.9	>−3.3	—	—	—
66811	0.45	2200±60	42400	1.3±0.1	3.0±0.2	4	yes	4	5.6±0.6	>−3.1	>−2.4	−3.3±0.1	−4.1±0.1	−3.2±0.2
149038	0.92	1750±100	30500	<0.24	—	4	?	—	<3.4	>−2.5	>−3.0	>−3.0	>−3.6	—
151804	1.90	1600±70	34000	0.4±0.1	0.4±0.1	4	probable	4	11.0±2.3	>−3.3	>−1.8	>−2.1	−3.8±0.3	—
190429A	2.6	2300±70	42400	<0.5	—	1	?	—	<35.4	>−4.0	>−2.7	>−4.1	—	>−4.2
210839	0.8	2100±60	38200	<0.4	—	2	?	—	<4.7	>−3.2	>−2.6	>−2.9	>−3.8	>−3.3

References: 1 Abbott et al. 1980; 2 Abbott et al. 1981, 3 Abbott 1985; 4 Bieging et al., 1989

[a] In calculating the error in $\dot{M}$ we took into account the error in S, v_∞ and a 10% error in D

[b] For ζ Pup and HD 151804 we used the mean value for $\dot{M}$, derived from the data at 6 and 2 cm

3. Comparison of observed and predicted ionization

3.1. Drew's models

Drew (1989) has calculated a number of ionization and thermal models for the winds of O-stars of luminosity class I, III and V. The input paramters such as $T_{\rm eff}$, R, $\dot{M}$ and v_∞ for the grid of wind models calculated by Drew are taken from Barlow (1986) with $v_\infty = 3v_{\rm esc}$. They are collected in Table 5. She adopted a slow velocity law with $\beta = 1$, which is higher than the value of $\beta \simeq 0.7$ appropriate for our stars (Paper I). She included the elements H, He, C, N, O, Ne, Mg, Si, S and Fe with the abundances given by Allen (1973), except for He for which she adopted $A_{\rm He} = 0.1$. Most metals were represented by their ground state only except C III, C IV, N III, N IV, O III, O IV and Si IV for which one (sometimes three) excited states were included.

The photoionization and excitation were calculated by assuming a mean intensity given by Eq. (A.2). The contribution by the diffuse field radiation, i.e. $B_\nu(T_e)$ in Eq. A.2, was approximated by $J_\nu = B_\nu(T_e)/b_1({\rm He}^+)$, where $b_1({\rm He}^+)$ represents the ground state departure coefficient of He^+. This approximation is only valid in the wavelength region where He^+ is the dominant source of opacity, that is between the absorption edge of He^+ at 54.4 eV and that of O IV at 77 eV. For higher energies this approximation of J_ν is only an upper limit. Drew claims that this is not important because she finds that photoionization by the diffuse radiation of species with thresholds larger than 77 eV is negligible.

The wind models calculated by Drew show that the electron temperature in the winds of O-stars is typically 0.5 to 0.6 $T_{\rm eff}$ at $v = 0.5\,v_\infty$. This is considerably lower than the values of $T_e \simeq 0.9\,T_{\rm eff}$ derived by Klein & Castor (1978) and adopted in many studies of the ionization in winds e.g. Olson & Castor (1981), Cassinelli & Olson (1979), Pauldrach (1987). Drew finds that the inclusion of heavy elements in the calculation of the thermal balance of the wind lowers the temperature substantially, because of the cooling due to radiative losses. This effect had already been noted by Krolik & Raymond (1985).

The value of $T_e \simeq 0.5$ to 0.6 $T_{\rm eff}$ in the wind is nearly independent of the input parameters: a change in the mass loss of a factor 5 changes T_e by at most 20%, a change of β from 1, the value adopted by Drew, to 0.7, the value found by us from UV line fitting (see Paper I), reduces T_e only in the inner part of the wind ($r \leq 1.3\,R_*$) by about 5%.

For the contribution by the stellar radiation field to J_ν Drew used the NLTE model fluxes of Mihalas (1972). For a few models she also calculated the ionization by adopting the fluxes from Kurucz (1979) LTE model atmospheres. This has little impact on T_e (4% cooler) but the degree of ionization changes drastically. Because of the relative deficiency of far UV flux in the Kurucz models, C V, N V and O V vanish in the wind, while trace species of the lower ionization stages like C III, N III, O III and Si IV are increased ten to hundredfold when LTE instead of the Non LTE model fluxes are used.

The stellar parameters for which Drew calculated the ionization in the winds are listed in Table 5. For these models she calculated the ionization balance of H, He, C, N, O, Ne, Mg, Si, S and Fe. She adopted a velocity law of $\beta = 1$ for all models. However, for C IV, N V and Si IV she also tabulated the values of $q(w)$ for other values of β. The predicted ionization will be compared with the observations in Sects. 3.3 and 3.4.

Table 4. Comparison of observed and predicted ionization balance for ζ Pup at $w=0.5$ and 0.9

	$w=0.5$			$w=0.9$		
	$\log q_{\mathrm{C\,III}}$	$\log q_{\mathrm{C\,IV}}$	$\log_{\mathrm{N\,V}}$	$\log q_{\mathrm{C\,III}}$	$\log q_{\mathrm{C\,IV}}$	$\log q_{\mathrm{N\,V}}$
Observed	>-3.9	>-3.1	>-2.4	>-4.1	>-2.4	>-1.9
Predicted[a]	-6.2	-1.9	-0.1	-4.0	-0.3	-2.3

[a] Pauldrach's (1987) model 3

Table 5. Input parameters for Drew's and Munich models

T_{eff}	$\log g$	$\log L/L_\odot$	$R/R_\odot$	$\dot{M}$ $(10^{-6}\,M_\odot\,\mathrm{yr}^{-1})$	v_∞ $(\mathrm{km\,s}^{-1})$	β	$\dot{M}/v_\infty R_*^2 \propto \bar{\rho}_w$ $(10^{-12}\,M_\odot\,\mathrm{yr}^{-1})/(R_\odot^2\,\mathrm{km\,s}^{-1})$
Drew's models[a]							
30000	3.0	5.48	20	0.48	1800	1	0.67
30000[b]	3.5	5.08	13	0.10	2900	1	0.20
30000[b]	3.5	4.73	8.5	0.026	3200	1	0.11
32500	3.3	5.61	20	0.83	1800	1	1.15
32500	3.8	5.23	13	0.18	2980	1	0.37
32500[b]	3.8	4.88	8.5	0.045	3200	1	0.19
35000	3.3	5.80	22	1.8	1800	1	2.07
35000	4.0	5.36	13	0.30	2900	1	0.61
35000	4.0	5.00	8.5	0.075	3200	1	0.32
37500	3.5	5.97	23	3.5	2300	1	2.88
37500	4.0	5.57	14	0.70	2900	1	1.23
37500	4.0	5.26	10	0.20	3200	1	0.63
40000	3.5	6.08	23	5.5	2300	1	4.53
40000	4.0	5.68	14	1.1	2900	1	1.94
40000	4.0	5.36	10	0.32	3200	1	1.00
45000	4.0	6.11	19	6.0	2900	1	5.73
45000	4.0	5.69	11	1.1	3200	1	2.84
50000	4.0	6.30	19	12	2400	1	13.8
50000	4.0	5.88	11	2.3	3000	1	6.34
55000	4.0	6.04	11	4.5	2500	1	14.9
Munich models							
32170	3.2	5.93	30	1.00	3150	0.90	0.35
34080	31.4	6.20	36.0	6.11	1951	0.83	2.42
35500	3.40	5.91	23.9	1.63	2724	0.85	1.05
35809	3.15	6.41	42.0	15.2	1401	0.86	6.15
38460	3.4	6.36	34.0	7.86	2584	0.79	2.63
39630	3.63	5.88	18.9	1.80	2826	0.80	1.78
40830	3.92	5.49	38	0.512	3630	0.81	0.10
42660	3.6	6.34	27.4	8.55	2929	0.79	3.89
45710	3.98	5.83	12.9	1.45	4560	0.79	1.91
51280	4.0	6.30	18.0	6.53	4490	0.81	4.49

[a] At each temperature Drew calculated three models representing luminosity class I, III, V. At 45 000 and 50 000 K the models represent LC I and V, the 55 000 K model represents a LC V star

[b] Model atmosphere fluxes used in these cases were calculated for a Hydrogen and Helium composition only

3.2. The Munich models

In this section we will describe the models kindly provided to us when the second author was a guest in Munich. These models were used by the Munich group to study the evolution of massive stars (Pauldrach et al. 1989). The physics of these models is described by Pauldrach (1987) and Pauldrach (1990). We will refer to these as the Munich-models. These models are isothermal with $T_e = T_{\mathrm{eff}}$.

For the caluclation of the photospheric radiation the LTE model atmospheres of Kurucz (1979) were used. The multilevel

Table 6. Comparison between the parameters of selected stars and the best-fitting model used for a detailed comparison of $\dot{M}q(w)$

Star/model	$\log g$	T(K)	$R/R_\odot$	$\log L/L_\odot$	$M/M_\odot$	v_{esc} (km s^{-1})	v_∞ (km s^{-1})	$\dot{M}(M_\odot\,\mathrm{yr}^{-1})$
HD 14947 O5If$^+$	3.7	40300	17.4	5.85	55	890	2300	
M C2	3.63	39600	18.5	5.88	54	836	2825	$1.80\,10^{-6}$
M C5	3.36	38300	22.7	6.00	43	535	2120	$4.20\,10^{-6}$
HD 46150 O5V((f))	4.0	44300	12.3	5.72	52	1090	2900	
M C1	3.98	45700	12.9	5.83	58	1093	4560	$1.45\,10^{-6}$
HD 101436 O6.5V	3.9	41200	12.3	5.60	44	1010	2800	
M D1	3.92	40830	11.2	5.49	38	1009	3630	$5.12\,10^{-7}$
HD 149038 O9.7Iab	3.21	30500	25	5.70	38	610	1750	
Drew O9 I	3.3	32500	20	5.61	30	600	1800	$8.3\,10^{-7}$
HD 37742 O9.7Ib	3.2	30500	26	5.74	41	620	2100	
M C4	3.2	32200	30	5.93	51	609	3150	$1.00\,10^{-6}$

statistical equilibrium equations are solved for 26 elements from H to Zn, including 133 ionization stages, 4000 levels and about 10 000 line-transitions. The continuum optical depth is represented by the photo-ionization from the ground levels of H, He, C, N, O, Ne, Mg, Si and S, by the free-free opacity of H and He and by electron scattering. Dielectronic recombination is considered for C III and N III only. The fact that dielectronic recombination is not included for many more ions may lead to significant errors in the ionization balance because the dielectronic recombination rates can be larger than the direct raidiative recombination rates (Aldrovandi & Pequignot 1973; Nussbaumer & Storey 1983).

Pauldrach (1987) finds that the inclusion of the excited levels in the calculation of the ionization balance in the winds is important. The low lying levels are collisionally excited and subsequently photoionized, resulting in a shift to higher ionization stages. For example, in the case of ζ Pup, O V is found to be the dominant ion, while O VI is formed by photo-ionization from excited O V levels. Pauldrach therefore concludes that Auger-ionization cannot be important in producing O VI, because Auger-ionization of the dominant O V ion would produce O VII instead of O VI. This conclusion is contrary to the one by Drew (1989) who found that Auger-ionization is necessary for the explanation of the observed fraction of O VI. The reason for this discrepancy is the fact that Drew's calculations show that T_e is much lower than the value of $T_e = T_{\mathrm{eff}}$ adopted by Pauldrach. At lower electron temperatures, typically $T_e \simeq 0.5\ T_{\mathrm{eff}}$, the collisional excitation is far less important than in Pauldrach's model and hence O VI cannot be formed by ionization from collisionally excited O V. Drew finds that O IV is the dominant stage of ionization, rather than O V. Therefore she concludes that Auger-ionization is needed to explain the superionization of O VI.

In Table 5 we have gathered the relevant data of the models provided by the Munich group. The value of β was calculated by us, fitting Eq. (5) to the velocity structure in the vicinity of $w = 0.5$.

3.3. Comparison between predicted and observed values of $\dot{M}q(w)$

In this section we compare the observed variation of the ionization balance with distance in the entire wind for several stars with the predicted values.

For this purpose we selected five representative program stars with well-determined values of $\dot{M}q(w)$. For each star we selected a model with approximately the same values of T_{eff} and $\log g$, and also similar values of L and R_*. The best-fitting models were chosen from the ten Munich models and the one model ($T_{\mathrm{eff}} = 32\,500$, $\log g = 3.3$) for which Drew (1989) gives the full radial dependence of the ionization. The five stars and their best-fitting models are listed in Table 6. Notice that the observed values of v_∞ are considerably smaller than the predicted values. This was discussed in Paper II.

The predicted ionization fractions, and the predicted mass loss rates were used to compare the predicted values of $\dot{M}q$ with the observed ones. We only did this for the resonance transitions C IV, N V, Si IV for which the excitation fraction $E \simeq 1$. Because the observed and theoretical terminal velocities differ we converted the radial coordinate to a velocity using Eq. (5) with the value of β of the observed star. The theoretical values and the observed values of $\dot{M}q$ for C IV, N V and Si IV as function of the normalised velocity w for the 5 stars are depicted in Fig. 5.

An inspection of this figure shows that the agreement between observation and theory is rather poor: in each of the five stars the predicted and observed values of $\dot{M}q$ differ by as much as a factor 10^2 or 10^3. We discuss these stars.

HD 14947 (O5If$^+$): The observed Si IV fraction is about 10^3 times higher than predicted. The lower limit to the observed C IV is in agreement with the predicted value.

HD 46150 (O5V((f))) and HD 101436 (O6.5V): The observed values of $\dot{M}q$(N V) are a factor 10^{-2} lower than predicted. The predicted and observed values of C IV agree within a factor three. The ionization fraction of C IV is about $5\,10^{-4}$ for HD 46150 and $7\,10^{-3}$ for HD 101436. The observed upperlimit for Si IV agrees with the predicted value.

HD 149038 (O9.7Iab): The predictions for this star are from Drew (1989). The observed values of N V and Si IV are a factor 10 to 10^2 higher than predicted at $w = 0.5$. The lower limit of C IV is in agreement with the observed value. The predictions indicate that C IV is expected to be the dominant stage of ionization.

HD 37742 (O9.7Ib): The predicted value for C IV is a factor 50 higher than observed. The predicted value for Si IV is a factor 5 lower than observed at $w = 0.5$. The observed value of N V is a factor 200 larger than predicted at $w = 0.5$. The predictions

indicate that C IV is the dominant stage of ionization, with q(C IV) larger than 0.95.

We conclude that:

i) For class V stars the observed upperlimits of Si IV agree with the theoretical predictions, but for class I stars the observed values of $\dot{M}q$ are larger than predicted. This underestimate of the predictions tends to increase from a factor 5 to 20 for O9.5 stars to a factor 10^3 for O5 stars.

ii) For the cooler stars (type O9.5) the theoretical models predict too much C IV by a factor of 50. However, this result is based on one star only. For stars of type O5–O7 there is a reasonable agreement between observed and predicted values of $\dot{M}q_{\mathrm{C\,IV}}$.

iii) The discrepancy between the observed and predicted value of $\dot{M}q_{\mathrm{N\,V}}$ shows the most striking behaviour. The predictions overestimate the N V abundance by a factor of 10 to 100 for stars of type O5–O7, but underestimate it by the same factor for O9 stars. This is the well known effect of superionization of N V which indicates that models which do not include Auger-ionization by X-rays fail to predict sufficient N V for the cooler stars.

We realize that these conclusions are based on a small number of stars. We are also aware of the possibility that different models with different ionization conditions can exist within the uncertainty of the stellar parameters. To elaborate this we checked if the stars in Table 6 could be compared to a second model with stellar parameters within the observational range of uncertainty. Only for HD 14947 could a second appropriate model be found: model C5 of Pauldrach et al. (1989). The stellar parameters of model C5 are listed in Table 6. The differences between the observed and model parameters of $\Delta \log g = 0.3$, $\Delta T_{\mathrm{eff}} = 2000$ K, $\Delta \log(R/R_\odot) = 0.12$, $\Delta \log(L/L_\odot) = 0.15$ are typical of the uncertainties in the observed quantities (see e.g. Paper I).

In Table 7 the observed values of $\dot{M}q(w=0.4)$ for HD 14947 are compared to the values of models C2 and C5. The table shows that the differences between models C2 and C5 are large, but the differences with the observed values remain. The predicted ionization fractions of N V and Si IV in model C5 agree better with the empirical fractions than model C2. However, the predicted C IV fraction does not agree with the observations.

Although part of the large differences between the observed and predicted ionization fractions, as discussed above, may be due to uncertainties in the stellar parameters, we do not believe this to be the general case. The differences discussed above are real and systematic as will be shown in the following section where we will compare the observed ionization ratios with the predicted ones for all our sample stars.

3.4. *Comparison between predicted and empirical ionization ratios*

The predicted and observed ionization ratios are compared with one another in Fig. 6. The predictions at $w=0.5$ are indicated by triangles (Munich) and crosses (Drew). The predicted ratios were calculated from the data in Fig. 5. The observed ratios at $w=0.5$ are shown by full lines. The areas covered by the upper and lower limits are indicated by hatched regions, in which arrows indicate whether these refer to upper or to lower limits. We discuss the different ratios separately.

i) N V/C IV There is a huge discrepancy between the observations and the predictions. At $\log T_{\mathrm{eff}} \lesssim 4.6$ this discrepancy is due to both an underestimate of N V and an overestimate of C IV (see

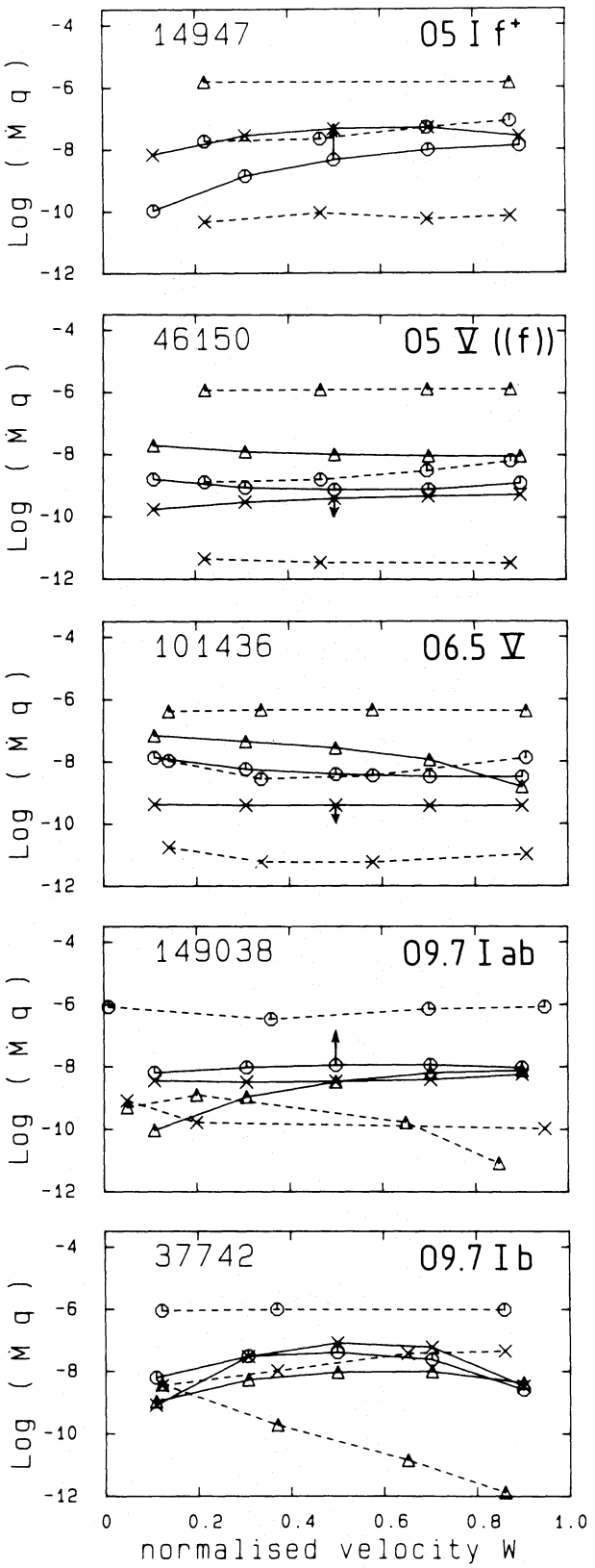

Fig. 5. Comparison between observed and predicted values of $\dot{M}q(w)$ in the entire wind. The solid line represents the observed values, the dashed lines the predictions of Drew or Pauldrach. We use the following symbols: C IV (○), N V (△), Si IV (×). Lowerlimits are indicated by an arrow of length 1.3 dex. Notice the large differences up to a factor 10^3 between theory and observations

Table 7. The influence of the uncertainty in the stellar parameters on the value of $\log \dot{M}q$ at $w=0.4$

		C IV	N V	Si IV
Star:	HD 14947	$-8.5<\cdots\leq-7.0$	-7.2^{a}	-7.4
Models:	M C2	-7.7	-5.8	-10.3
	M C5	-5.8	-6.8	-8.8

[a] This value is not derived from a detailed fit because the spectrum below 1240 A is extremely noisy. This value was determined by comparing the emission part of the N V doublet to other stars

Sect. 3.3). For $\log T_{\rm eff}>4.6$ the theoretical models predict a larger ratio than observed. This is due to an overestimate of N V.

ii) Si IV/C IV The observed ratio in the winds of supergiants is about a factor 1000 larger than predicted. For $4.50\lesssim\log T_{\rm eff}\lesssim4.60$ this is due to an underestimate of Si IV by a factor of 20 and an overestimate of C IV by a factor of 50; for $\log T_{\rm eff}\gtrsim4.60$ this is due to an underestimate of Si IV by a factor of 1000 (see Sect. 3.3). For the coolest stars ($\log T_{\rm eff}\lesssim4.50$) Drew predicted a strong dependence of the Si IV/C IV ratio on luminosity. Unfortunately, however, the predictions for the class I stars give the lowest values of Si IV/C IV. The observed upperlimits for class III and V stars do not disagree with the predictions.

iii) N V/Si IV For the late O and B0 supergiants the predictions agree well with the observations. Because both the N V/C IV and Si IV/C IV ratio show the same behaviour, this agreement shows that the predicted values of N V and Si IV are underestimated by about the same factor. This is confirmed by the conclusions of Sect. 3.3. For the hotter stars we expect the N V/Si IV ratio to be higher than observed because of the overestimate of N V. This is confirmed in Fig. 6c.

iv) C III/Si IV The comparison between the observations and theory is complicated by the fact that the observations refer to qE(C III′), i.e. the abundance of the excited level, whereas the predictions refer to the ionization fraction q(C III). Considering the fact that the excitation factor E(C III′) is less than one, we find that the observed C III/C IV ratio for stars with $\log T_{\rm eff}\lesssim4.55$ is higher than predicted by at least a factor 10^1. This is due to an overestimate of C IV, and therefore an underestimate of C III. At $\log T_{\rm eff}\gtrsim4.55$ the observed upperlimits do not disagree with the predictions.

v) N IV/N V The comparison between predictions and observations are complicated by the fact that the observations refer to qE(N IV′) whereas the predictions refer to q(N IV). The large discrepancy between the high predicted values of N IV/N V and the much lower observed values of N IV′/N V are partly due to the unknown excitation factor E(N IV′). However, considering the behaviour of N V described in Sect. 3.3, we believe that the large predicted ratios are due to an underestimate of the ionization fraction of N V, especially for the cooler stars with $\log T_{\rm eff}\lesssim4.55$. This implies that the excitation fraction is $E(\text{N IV}')\lesssim10^{-1}$, assuming that the underestimate of N V equals the overestimate of N IV and using the results of Sect. 3.3. For the hotter stars, using the same argument together with the result of Fig. 5e that $q(\text{N IV})/q(\text{N V})_{\rm PRED}\simeq10qE(\text{N IV}')/q(\text{N V})_{\rm OBS}$ we estimate that $E(\text{N IV}')\simeq10^{-3}-10^{-4}$.

The discrepancy between the observations and Drew's models cannot be resolved by using the results for the more appropriate value $\beta=0.7$ in the velocity law. For example this would raise the N V/C IV ratio by at most 0.8 dex and the Si IV/C IV ratio by 0.2 dex, whereas the discrepancy is a factor 10 to 1000.

We conclude that the conclusions derived in Sect. 3.3 for a few stars only, are strengthened by considering all our sample stars.

4. Discussion and conclusions

In this paper we have studied the general trends of the ionization fractions and ionization ratios in the winds of O-stars. The ionization was derived from the linefitting of the UV lines of 26 O-stars and 1 B-star by means of the SEI-method (Paper I). The empirical trends are compared with predicted trends to test the accuracy of stellar wind models.

The empirical ionization of the observed ions is expressed in terms of the product $\dot{M}qE$, where $\dot{M}$ is the mass loss rate and q and E are the ionization and excitation fractions in the wind at a distance where $v=0.5\,v_\infty$, or in terms of the ionization ratios q_i/q_j of different ions at $v=0.5\,v_\infty$. The empirical ionization ratios seem to correlate with $T_{\rm eff}$ (Fig. 3) in the general trends. These empirical trends are described by Eq. (6). The scatter in the trends is probably due to differences in wind-density and/or mass loss rates for stars of the same temperature. The trends describe the sensitivity of the ionization to $T_{\rm eff}$ and can be compared with predicted ionization in the winds of O-stars. For a detailed comparison of empirical and predicted ionization on a star to star basis, the ionization data in Table 5 should be used, or the results of the linefits published in Paper I.

The ionization fractions in terms of $\dot{M}qE$ and the ionization ratios q_i/q_j are compared with predictions of the stellar wind models of Drew (1989) which include radiative cooling by metal lines, and those by Pauldrach (1987) and Pauldrach et al. (1989) which include a full Non-LTE treatment of 133 ions. Drew's models are significantly cooler ($T_e\sim0.6\,T_{\rm eff}$) than the value of $T_e=T_{\rm eff}$ adopted by the Munich group. In Drew's models the energy balance is calculated accurately, but the population of the excited levels is not calculated accurately. On the other hand the Munich models treat excited levels consistently but the wind is assumed to be isothermal at $T_e=T_{\rm eff}$. Both models neglect the possibility of photoionization from X-rays created in shocks in the wind.

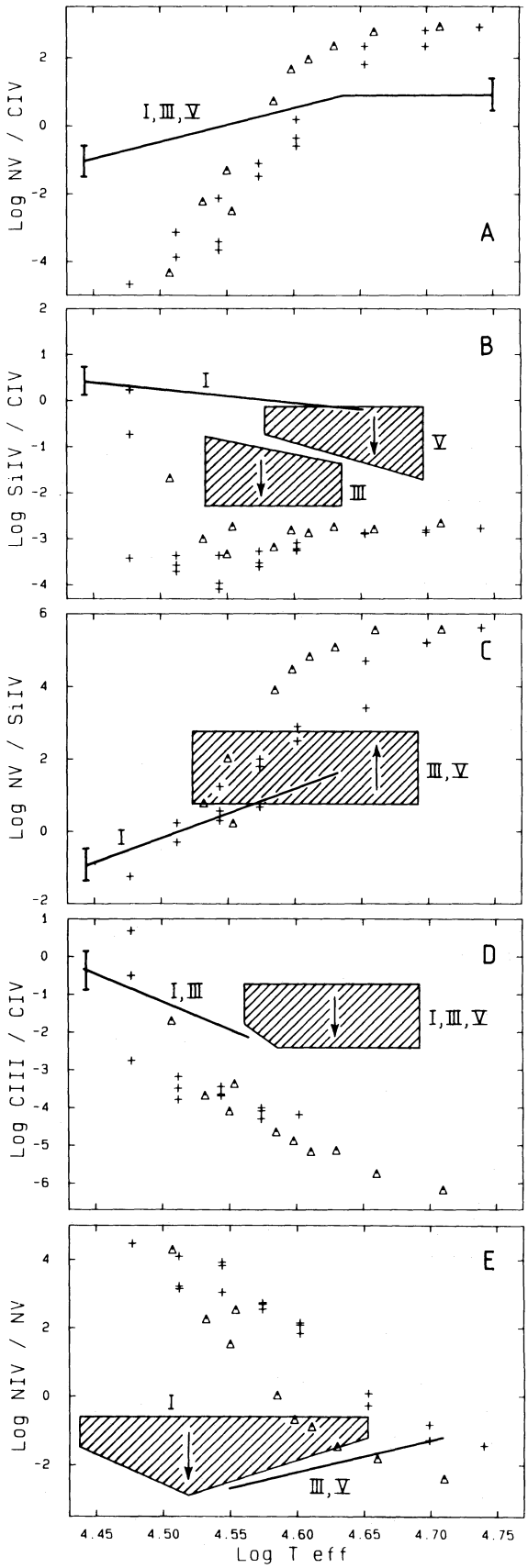

Fig. 6. Comparison between predicted and observed ionization ratios at $w=0.5$. Predicted ratios following Drew's (+) or Munich models (△). The observed ratios are indicated by full lines and the upper or lower limits are indicated by the hatched areas. Notice the large differences up to factors 10^3 between theory and observations

Both sets of models fail to explain the observations drastically (Figs. 5 and 6). Especially the N V/C IV and Si IV/C IV ratios indicate the failure of the theoretical predictions to fit the observations. For the early O-stars with $T_{\rm eff} \gtrsim 40\,000$ K the predicted N V/C IV ratio is larger than observed by a factor 10^1 to 10^2. The results discussed in Sect. 3.4 indicate that this is due to an overestimate of the predicted ionization fraction of N V in these stars. For cooler stars with $T_{\rm eff} \lesssim 40\,000$ K the predicted N V/C IV ratio is much smaller than observed by a factor which decreases from 10^{-2} at $\log T_{\rm eff} \simeq 4.55$ to 10^{-4} at $\log T_{\rm eff} \simeq 4.50$. This is due to a severe underestimate of the predicted ionization of N V and an overestimate of the predicted amount of C IV. For the O supergiants with $T_{\rm eff} \lesssim 40\,000$ K the predicted Si IV/C IV ratio is smaller than predicted by about a factor 10^{-3}. This is due to an underestimate of the amount of Si IV and an overestimate of C IV.

Part of the discrepancies shown in Fig. 5 between predicted and empirical ionization ratios might be solved by selecting models with slightly different stellar parameters. However, the trends in Fig. 6 show that the discrepancies are large and systematic, and that they cannot be solved by ad-hoc changes of the model parameters.

The large discrepancies between the predicted and observed ionization in the winds of O-stars reported in this paper might seem to contradict the statement by Pauldrach et al. (1989) that the predicted UV lines of O stars agree quantitatively with the observed lines. However, a quick glance at the profiles predicted by Pauldrach et al. shows that the agreement is only qualitatively, and that large quantitative differences between the observed and predicted profiles exist. Our empirical profiles obtained by detailed line-fitting agree an order of magnitude better with the observations than those predicted by Pauldrach et al. Therefore it is not surprising that we find large differences between the empirical and the predicted ionization.

The large discrepancies between theory and observations indicate that the present theoretical wind models are not as good as one might hope. Possible sources for the failure of the theoretical ionization could be: the errors in the treatment of the excited levels in Drew's models; the possible error in the assumed isothermal structure of $T_e = T_{\rm eff}$ in the Munich models; the neglect of Auger ionization by X-rays created by shocks in the winds of O-stars.

A model to calculate the ionization balance in the wind including a non-isothermal wind structure, photoionization from excited levels and inner shell photoionization from X-rays is being constructed by one of us (MG) in Utrecht.

Appendix A

Why do the ionization ratios mainly depend on T_{eff}?
Neglecting for simplicity collisional ionization and photoionization from excited levels the ionization equilibrium between two successive stages of ionization is expressed as:

$$n_z/n_{z+1} = n_e\alpha \Big/ \int \frac{4\pi}{h\nu} J_\nu \sigma_\nu \, d\nu \qquad \text{(A.1)}$$

where n_e is the electron density, α is the recombination efficient, and σ_ν is the absorption coefficient for photoionization, and J_ν is the mean intensity. The mean intensity J_ν can be approximated by

$$J_\nu = W \cdot F_\nu^* \, e^{-\theta_\nu} + B_\nu(T_e) \qquad \text{(A.2)}$$

where W is the geometrical dilution factor, F_ν^* is the photospheric flux at the stellar surface and θ_ν is the optical depth of the wind between the photosphere and the distance where the ionization is calculated.

The first term in Eq. (A.2) is the contribution by the photospheric radiation and the second term the locally generated radiation. Let us first consider the case that the ionization edge of an ionization species, z, lies in the optically thin part of the wind. Then the first term in Eq. (A.2) dominates the second one. Replacing the photospheric flux by a black body with temperature $T_{\rm eff}$ we get

$$\frac{n_z}{n_{z+1}} = n_e \alpha \Big/ \left(\frac{8\pi W k^3 T_{\rm eff}^3}{c^2 h^3} \int_{x_0}^{\infty} \frac{x^2}{e^x - 1} dx \right) \tag{A.3}$$

with $x_0 = h\nu_0 / kT_{\rm eff}$ and ν_0 the frequency corresponding to the ionization potential. For typical ions of interest $h\nu_0$ is in the range 30–50 eV, while $kT_{\rm eff} < 4.3$ eV for $T_{\rm eff} < 50\,000$ K, so $x_0 \gtrsim 10$. Neglecting therefore the -1 in the integrand and integrating by parts we get

$$n_z / n_{z+1} = n_e \alpha \Big/ \left(\frac{8\pi W k^3 T_{\rm eff}^3}{c^2 h^3} (x_0^2 + 2x_0 + 2) e^{-x_0} \right) \tag{A.4}$$

neglecting the term $2x_0 + 2$ compared to x_0^2 (accurate to 25%) we finally get

$$n_z / n_{z+1} \sim (n_e / W) e^{(h\nu_0 / kT_{\rm eff})} / T_{\rm eff}$$

or

$$\log (n_z / n_{z+1}) \sim \log \overline{\rho_w} + \frac{\text{constant}}{T_{\rm eff}} - \log T_{\rm eff} \tag{A.5}$$

where we defined $\overline{\rho_w} = \dot{M} / (v_\infty R^2)$ which is proportional to n_e (compare this expression to the one derived by Pauldrach et al. 1989). We see that the ionization fraction depends on $T_{\rm eff}$ and the mean density $\bar{\rho}_w$. However, $\bar{\rho}_w$ is also a strong function of $T_{\rm eff}$ as we will show. It is well established that the mass loss rate is primarily a function of luminosity (see e.g. Howarth & Prinja 1989), and that the terminal velocity is a strong function of the escape velocity (see e.g. Paper II). Therefore we have

$$\overline{\rho_w} \equiv \frac{\dot{M}}{v_\infty R^2} \sim \frac{L^\gamma}{v_{\rm esc} R^2} \sim \frac{(R^2 T_{\rm eff}^4)^\gamma}{\sqrt{2gR}\, R^2} \sim R^{2\gamma - 5/2} g^{-1/2} T_{\rm eff}^{4\gamma}. \tag{A.6}$$

To investigate this further we calculated $\bar{\rho}_w$ for the models of Drew (1989) and Pauldrach et al. (1989) which will be used to compare observed and predicted variation fractions in Sect. 3. The results are in the last column of Table 5.

Drew has used $\gamma = 1.72$ and $v_\infty / v_{\rm esc} = 3.0$ so we expect $\bar{\rho}_w \sim R^{0.94} g^{-1/2} T_{\rm eff}^{6.88}$, to be a strong function of $T_{\rm eff}$. This is indeed confirmed. For a given $T_{\rm eff}$ the variation in $\bar{\rho}_w$ is less than a factor 5.

For the Munich models the situation is less obvious. Pauldrach et al. (1989) report that the mass loss rates they derive, show approximately the same luminosity dependence as found by Howarth & Prinja (1989): $\gamma \simeq 1.6$. Therefore we expect $\overline{\rho_w} \sim R^{0.7} g^{-1/2} T_{\rm eff}^{6.4}$. This means that the temperature dependence is again very pronounced. Furthermore, the ratio $v_\infty / v_{\rm esc}$ in the models varies from 1.5 to 3.9. This means that the constant of proportionality in Eq. (A.6) is not constant as in Drew's case, but varies by more than a factor 2.

So if the wind is optically thin for the frequency edge of ion z, then the ratio n_z / n_{z+1} will be a strong function of $T_{\rm eff}$ and a much weaker function of the stellar gravity. In the case that the wind is optically thick at the ionization edge of ion z the situation becomes more complicated. The diffuse radiation field will play a role [the second term in Eq. (A.2)] as well as photoionization from excited levels. In that case, the ionization fractions will be a function of $T_{\rm eff}$ and density. However, we have shown above that the density is expected to be a strong function of $T_{\rm eff}$. So the ionization fraction will depend mainly on $T_{\rm eff}$.

References

Abbott D.C., Bieging J.H., Churchwell E., Cassinelli J.P., 1980, ApJ 238, 196
Abbott D.C., Bieging J.H., Churchwell E., 1981, ApJ 250, 645
Abbott D.C., Bieging J.H., Churchwell E., 1984, ApJ 280, 671
Abbott D.C., 1985, in: Radio Stars, eds. R. Hjellming, D. Gibson, Reidel, Dordrecht
Aldrovandi S.M.V., Pequignot D., 1973, A&A 25, 137
Allen C.W., 1973, Astrophysical Quantities, Athlone Press, London
Baade D., Lucy L.B., 1987, A&A 178, 213
Barlow M.J., 1987, in: Proc. 4th British–Spanish School in Astrophysics: Massive Stars, ed. M. Moles
Bieging J.H., Abbott D.C., Churchwell E., 1989, ApJ 340, 518
Carlberg R.G., 1980, ApJ 241, 1131
Cassinelli J.P., Olson G.L., Stalio R., 1978, ApJ 220, 573
Cassinelli J.P., Olson G.L., 1979, ApJ 229, 304
Cassinelli J.P., Waldron W.L., Sanders W.T., Harnden F.R., Rosner R., Vaiana G.S., 1981, ApJ 250, 677
Cassinelli J.P., Swank J.H., 1983, ApJ 271, 681
Chlebowski T., Garmany C.D., 1989 (private communication)
Drew J., 1989, ApJS 71, 267
Garmany C.D., 1987 (private communication)
Groenewegen M.A.T., Lamers H.J.G.L.M., 1989a, A&AS 79, 359 (Paper I)
Groenewegen M.A.T., Lamers H.J.G.L.M., Pauldrach A., 1989b, A&A 221, 78 (Paper II)
Hamann W.R., 1981, A&A 93, 353
Harnden F.R., Branduardi G., Elvis M., Gorenstein P., Grindlay J., Pye J.P., Rosner R., Topka K., Vaiana G.S., 1979, ApJ 234, L51
Howarth I., Prinja R.K., 1989, ApJS 69, 527
Klein R.I., Castor J.I., 1978, ApJ 220, 902
Krolik J.H., Raymond J.C., 1985, ApJ 248, 660
Kurucz R.L., 1979, ApJS 40, 1
Lamers H.J.G.L.M., Morton D.C., 1976, ApJS 34, 715
Lamers H.J.G.L.M., Rogerson J.B., 1978, ApJ 66, 417
Lamers H.J.G.L.M., Snow T.P., 1978, ApJ 219, 504
Lamers H.J.G.L.M., Cerruti-Sola M., Perinotto M., 1987, ApJ 314, 726
Long K.S., White R.L., 1980, ApJ 239, L65
Lucy L.B., Solomon P.M., 1970, ApJ 159, 879
Lucy L.B., 1982, ApJ 255, 268
Lucy L.B., 1984, ApJ 284, 351
MacGregor K.B., Hartmann L., Raymond J., 1979, ApJ 231, 514
Maeder A., Meynet G., 1987, A&A 182, 243
Martens P.C.H., 1979, A&A 75, L7
Mihalas D., 1972, NCAR technical note, STR-76
Nussbaumer H., Storey P.J., 1983, A&A 126, 75

Olson G.L., 1978, ApJ 226, 124
Olson G.L., Castor J.I., 1981, ApJ 244, 179
Owocki S.P., Rybicki G.B., 1984, ApJ 284, 354
Owocki S.P., Rybicki G.B., 1985, ApJ 299, 265
Owocki S.P., Rybicki G.B., 1986, ApJ 309, 127
Owocki S.P., Castor J.I., Rybicki G.B., 1989, ApJ (submitted)
Palme H., Suess H.E., Zeh H.D., 1982, in: Landolt-Bornstein, new series, group VI, vol. 2b, eds. K. Schaiffer, H.H. Voight, Springer, Berlin Heidelberg New York
Pauldrach A.W.A., 1987, A&A 183, 295
Pauldrach A.W.A., Kudritzki R.P., Puls J., Butler K., 1990, A&A 228, 125
Pauldrach A.W.A., 1990 (preprint)
Snow T.P., Morton D.C., 1976, ApJS 32, 429
Walborn N.R., Nichols-Bohlin J., Panek R.J., 1985, NASA reference publication 1155: International Ultraviolet explorer atlas of O-type spectra from 1200 to 1900 Å
Waldron W.L., 1984, ApJ 282, 256
Wright A.E., Barlow M.J., 1975, MNRAS 170, 41